GENERAL MEDICAL APPLICATIONS OF STRUCTURE-AIDED DRUG DESIGN

Acta Cryst. (1995). D51, 590–596

Crystallographic and Thermodynamic Comparison of Structurally Diverse Molecules Binding to Streptavidin

BY PATRICIA C. WEBER*

The DuPont Merck Pharmaceutical Company, PO Box 80228, *Wilmington, DE* 19880-0228, *USA*

AND MICHAEL W. PANTOLIANO AND F. RAYMOND SALEMME

3-*Dimensional Pharmaceuticals, Inc.*, 665 *Stockton drive, Suite* 104, *Exton, PA* 19341, *USA*

(*Received* 24 *August* 1994; *accepted* 27 *January* 1995)

Abstract

Crystallographic structures and thermodynamic binding parameters are compared for three structural classes of streptavidin ligand including d-biotin, 2-[(4′-hydroxyphenyl)-azo] benzoate and the peptide NH_2-Phe-Ser-His-Pro-Gln-Asn-Thr-COOH. Descriptions of these structural and thermodynamic observations emphasize the diversity of potential strategies for improving ligand affinity.

Introduction

Structure-based drug design uses the three-dimensional structure of a lead compound complexed with a target enzyme or receptor to direct the chemical elaboration of drugs with high potency and specificity. Although many successes have been reported using structure-based methods (*e.g.* Appelt *et al.*, 1991; Erion *et al.*, 1993; Weber, Pantoliano, Simons & Salemme, 1994), few general rules have emerged that represent consistently reliable strategies for improving the binding affinity of lead compounds. In large part this situation reflects the complexity of interpreting three-dimensional structures of protein–ligand complexes in terms that allow the reliable manipulation of the free energy of ligand binding.

In the present work, the thermodynamic binding parameters and crystallographic structures are compared for streptavidin complexed with three structurally distinct classes of ligand (Fig. 1). These include d-biotin [the natural ligand for streptavidin (Chaiet & Wolf, 1964)], 2-[(4′-hydroxyphenyl)-azo]benzoate [HABA, an azobenzene dye used to quantitate the concentration of biotin-binding sites in solutions of avidin and streptavidin (Green, 1965)] and a streptavidin-binding peptide (NH_2-Phe-Ser-His-Pro-Gln-Asn-Thr-COOH) whose sequence was discovered by random screening approaches using both phage library (Devlin, Panganiban & Devlin, 1990) and solid support display methods (Lam *et al.*, 1991). For two classes of ligand, we describe examples of modified forms that have enhanced affinity. This comparison of three ligand classes demonstrates that experimental knowledge of the thermodynamic ligand-binding parameters provides insights that are key to the energetic evaluation of structural features and can help define improved strategies for increasing ligand affinity.

Experimental

Ligand-binding measurements

The thermodynamic binding parameters for azobenzene dyes and the peptides were determined using isothermal titration calorimetry. The peptide (NH_2-Phe-Ser-His-Pro-Gln-Asn-Thr-COOH) was synthesized on an Applied Biosystems peptide synthesizer and purified by high pressure liquid chromatography (Weber, Pantoliano & Thompson, 1992). 3′,5′-dimethyl HABA was synthesized by coupling diazotized 4-aminobenzoic acid to 2,6-dimethyl phenol. Lyophilized streptavidin (*Streptomyces avidinii* streptavidin, Calbiochem, La Jolla, CA) was dissolved in unbuffered 100 m*M* KCl. This avoids heat effects due to ionization of buffer components during the titration experiment. The solution pH was adjusted using small amounts of 1 *M* NaOH and 1 *M* HCl and the protein was equilibrated with this solution by dialysis. A control experiment diluting the ligand into 0.1 *M* KCl solution was performed to correct for small contributions of heat of dilution. The solid ligands were dissolved in the dialyzate that resulted from the streptavidin dialysis to insure composition identity with respect to all solution components other than the reactants.

As described in detail elsewhere (Weber *et al.*, 1994; Weber, Pantoliano *et al.*, 1992; Weber, Wendoloski, Pantoliano & Salemme, 1992), streptavidin solutions were titrated by addition of 15 µl aliquots of ligand solution at 299 K using a MicroCal Omega titration calorimeter (Northampton, MA). The binding parameters, K_a, ΔH° and n (stoichiometry per subunit) were obtained through non-linear least-squares fit of the observed reaction heat for each titration step (Wiseman, Williston, Brandts &

*Current address: Schering-Plough Research Institute, 2015 Galloping Hill Road, K-15-3-3855, Kenilworth, NJ 07033-0539, USA.

Lin, 1989). The ligand concentration was ten times higher than the streptavidin concentration to ensure that at least 80% of the ligand per injection was bound to the protein for the first few injections. Moreover, these conditions also ensured that at least 80% of the binding sites would be saturated after the last injection so that the binding reaction was followed over a wide range of fractional saturation.

The affinity of 5-([*N*-(5-{*N*-[6(biotinoyl)amino]-hexanoyl}-amino)-pentyl]-thioureidyl)-fluorescein, a molecule having the fluorescein and biotin moieties linked by a relatively long aliphatic chain, [fluorescein biotin (BTF), Molecular Probes Inc., Eugene, Oregon, USA] was determined by differential scanning calorimetric (DSC) measurements, where the observed melting temperature of the protein–ligand complex can be used to estimate the ligand association constant (Brandts & Lin, 1990). DSC measurements were performed with a Hart 7707 DSC heat conduction scanning microcalorimeter incorporating two matched pairs of removable ampoules. Lyophilized streptavidin was dissolved in 0.1 *M* piperazine-*N*,*N*′-bis(2-ethane sulfonic acid) (PIPES), pH 7.0 in presence of a twofold molar excess of ligand per subunit. Final ampoule protein concentrations were approximately 5×10^{-3} *M* as determined by amino-acid composition analysis. Using the scanning procedure previously described (Weber *et al.*, 1994), the T_m for the streptavidin–BTF complex was measured as the midpoint in the unfolding transition. The thermodynamic and binding parameters determined for streptavidin ligands are given in Table 1.

Crystallographic studies

X-ray diffraction experiments were carried out with a crystal form of streptavidin (Pahler, Hendrickson, Kolk, Argarana & Cantor, 1987) in which the biotin-binding sites are accessible to solvent channels so that ligands can be diffused into the crystal where complex

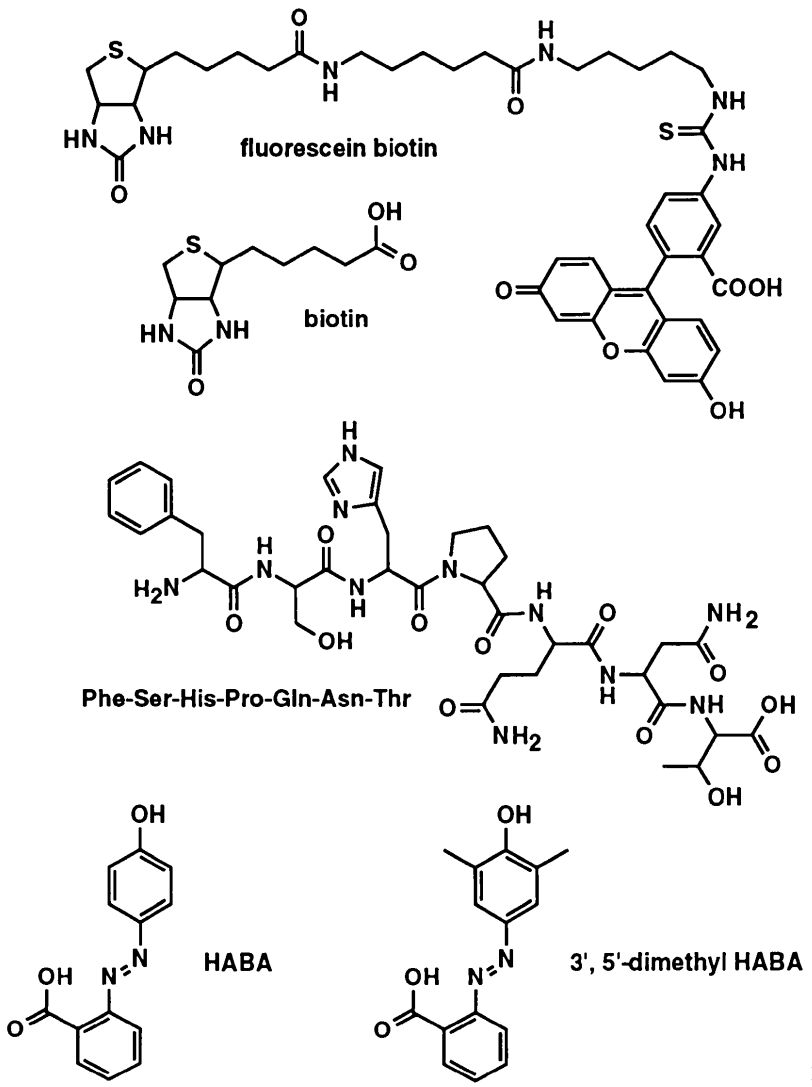

Fig. 1. Chemical structures of streptavidin ligands.

Table 1. *Thermodynamic parameters for molecules binding to streptavidin*

Ligand	K_a (M^{-1})	$\Delta G°$ (kcal mol^{-1})*	$\Delta H°$ (kcal mol^{-1})*	$T\Delta S°$ (kcal mol^{-1})*
Biotin†	2.5×10^{13}	−18.3	−32.	−13.7
Biotin–fluorescein‡	1.6×10^{14}	−19.4		
2-[(4′-hydroxyphenyl)-azo]benzoate (HABA)§	7300	−5.27	+1.70	+6.97
2-[(4-hydroxy,3′,5′-dimethylphenyl)-azo]benzoate (3′,5′-dimethyl-HABA)§	1200000	−8.29	+2.15	+10.44
NH_2-Phe-Ser-His-Pro-Gln-Asn-Thr-COOH¶	7944	−5.32	−19.34	−14

* 1 kcal mol^{-1} = 4.184 kJ mol^{-1}.

† Only $\Delta H°$ was fitted for the observed reaction heat with K_a fixed at the literature value of 2.5×10^{13} M^{-1} (Green, 1975).

‡ For a tight binding system of stoichiometry 1:1 in which there is one unfolding transition, one can estimate the binding constant at T_m from the following expression (Brandts & Lin, 1990), $K_a^{T_m} = \{\exp -(\Delta H_u/R)[(1/T_m) - (1/T_0)] + (\Delta C_{pu}/R)\ln[(T_m/T_0) + (T_0/T_m) - 1]\}/[L]_{T_m}$, where $K_a^{T_m}$ = the ligand association constant at T_m. (T_m values for streptavidin complexed with biotin and biotin–fluorescein were 395.8 and 398.9 K, respectively.) T_m = midpoint for protein unfolding transition in presence of ligand. T_0 = midpoint for protein unfolding transition in absence of ligand. (T_0 = 357.25 K for unliganded streptavidin.) ΔH_u = enthalpy of protein unfolding in absence of ligand T_0 (ΔH_u = 80.0 kcal mol^{-1}). ΔC_{pu} = change in heat capacity upon protein unfolding in absence of ligand (ΔC_{pu} = 0.95 kcal mol^{-1}K). $[L]T_m$ = free ligand concentration at T_m. R = gas constant.

§ Weber, Pantoliano, Simons & Salemme (1994).

¶ Weber, Pantoliano & Thompson (1992).

Table 2. *Summary of crystallographic refinement statistics for streptavidin–ligand complexes*

	Biotin–fluorescein	FSHPQNT*	HABA†	Dimethyl HABA‡
Space group	*I*222	*I*222	*I*222	*I*222
Unit-cell dimensions				
a (Å)	95.2	95.2	95.2	95.6
b (Å)	106.5	106.6	106.5	106.5
c (Å)	47.9	47.9	47.9	48.9
Resolution range (Å)	10–1.8	10–2.0	10–1.78	10–1.65
Number of reflections	14089	15592	17650	24078
R factor	0.181	0.179	0.181	0.175
R.m.s. deviations				
Bond distance (Å)	0.019	0.025	0.014	0.024
Angle distance (Å)	0.029	0.039	0.026	0.035
Planar group distance (Å)	0.013	0.017	0.013	0.015
Chiral volumes (Å^3)	0.231	0.327	0.194	0.289
Protein Data Bank code	1STP	1PTS	1SRE	1SRI

* Weber *et al.* (1992).

† Weber, Wendoloski, Pantoliano & Salemme (1992).

‡ Weber *et al.* (1994).

formation can occur. Orthorhombic crystals (space group *I*222, one dimer per asymmetric unit) of apostreptavidin were typically soaked for at least 24 h in saturating concentrations of ligand to prepare complex crystals.

X-ray diffraction data for complex crystals were collected using a Siemens imaging proportional counter and reduced to integrated intensities using *XENGEN* data-reduction software (Howard *et al.*, 1987). Crystals were stable in the X-ray beam and one crystal was used to collect a complete data set for each complex.

The structures of streptavidin–ligand complexes were refined at high resolution using restrained least-squares methods (Hendrickson & Konnert, 1980; Finzel, 1987), alternating with manual rebuilding cycles into $(F_o - F_c)\alpha_{calc}$ and $(2F_o - F_c)\alpha_{calc}$ electron-density maps (Jones, 1978). Chemically identical monomers in the crystallographic asymmetric unit were refined independently, starting with ligand-free models. Solvent molecules were introduced as they emerged as peaks greater than 3σ from the $(F_o - F_c)\alpha_{calc}$ electron-density maps during successive refinement cycles. In the crystal structures of the biotin and BFT complexes with streptavidin, residues of the protein structure corresponding to 'core' streptavidin (residues 13–138, Pahler *et al.*, 1987) are well defined in the electron-density maps. When complexed with either the azobenzene dye or peptide ligands, loop residues 47–52 and 66–68 and carboxy terminal residues 134–138 are less well ordered and in some cases are not included in the protein model. The electron density maps were sufficiently clear to unambiguously define the orientation of the various ligands, although only relatively weak electron density was found for both terminii of the peptide and the fluorescein portion of BTF. Crystallographic statistics for the streptavidin–ligand complexes are listed in Table 2.

Results

Streptavidin structure

Streptavidin is isolated as a tetramer of identical subunits which, in both the unliganded and liganded forms, are arranged with 222 tetrahedral symmetry (Weber, Ohlendorf, Wendoloski & Salemme, 1989). Each subunit is folded into an eight-stranded antiparallel β-barrel. The biotin-binding site is located at one end of each barrel in a pocket lined by amino-acid side chains from the interior of the β-barrel and from a loop of a symmetry-related subunit.

Biotin–streptavidin and biotin-fluorescein–streptavidin interactions

Streptavidin binds biotin with exceptionally high affinity ($K_a \simeq 10^{13}\,M^{-1}$, Green, 1975). Multiple interactions are formed between biotin heteroatoms and the aromatic and polar amino-acid side chains lining the biotin-binding pocket (Fig. 2*a*). These interactions include numerous van der Waals packing interactions with tryptophan indole side chains lining the pocket, an extensive pattern of hydrogen bonds with the biotin

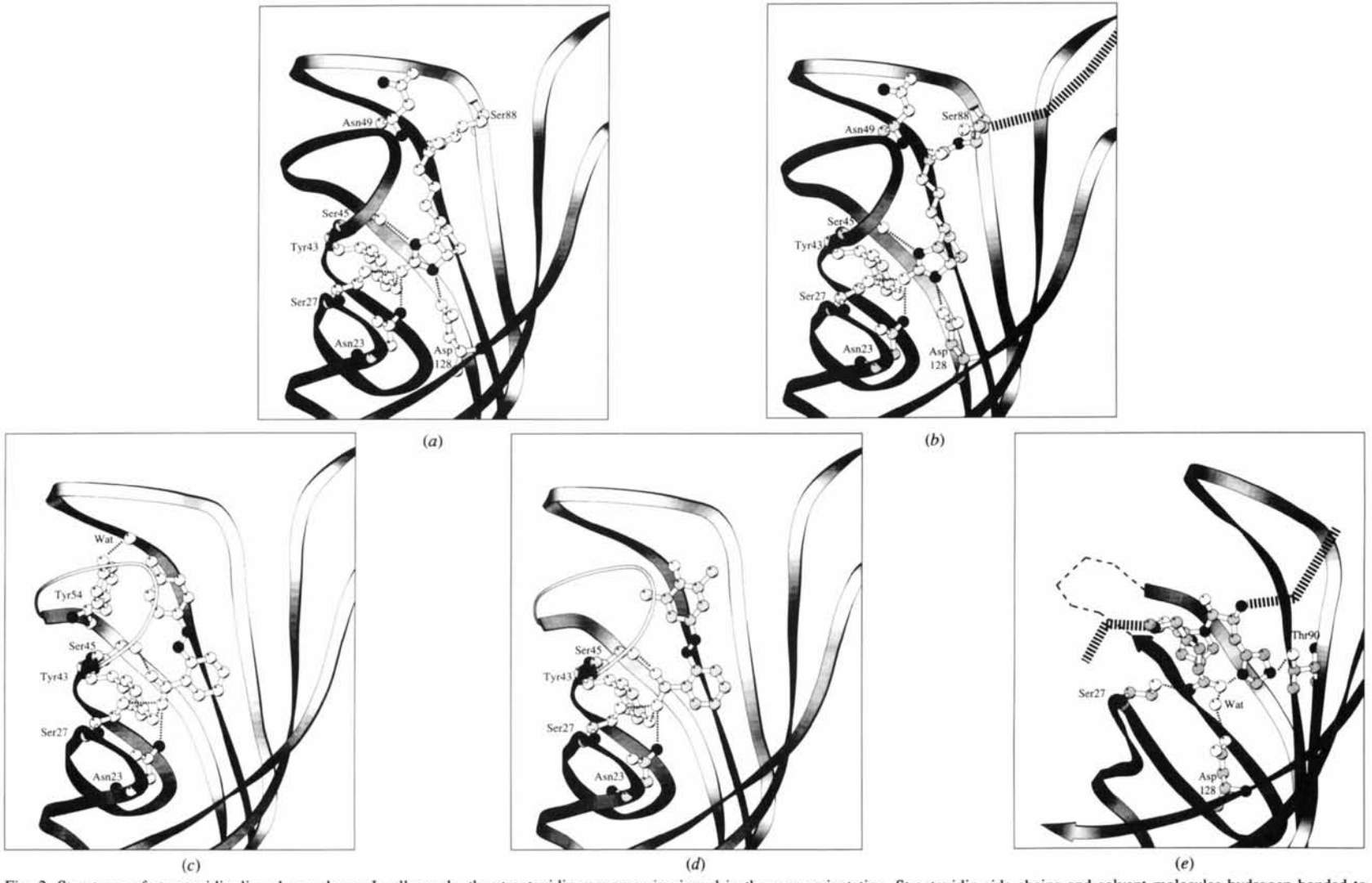

Fig. 2. Structures of streptavidin–ligand complexes. In all panels, the streptavidin monomer is viewed in the same orientation. Streptavidin side chains and solvent molecules hydrogen bonded to the ligand and the ligand atoms are shown in a ball-and-stick representation where C, O and N atoms are colored grey, white and black, respectively. Small dashed lines indicate hydrogen bonds. The streptavidin backbone structure is represented by ribbons (*MOLSCRIPT*, Kraulis, 1991). (*a*) Biotin–streptavidin complex. (*b*) Fluorescein biotin–streptavidin complex. Wide dashed lines indicate approximate location of atoms linking biotin and fluorescein. Fluorescein moiety is not defined in the electron-density maps. (*c*) and (*d*) HABA–streptavidin and 3′,5′-dimethyl HABA–streptavidin complexes. Position of residues 46–51, which are poorly defined in the electron density is shown as a thin ribbon. (*e*) (NH_2-Phe-Ser-His-Pro-Gln-Asn-Thr-COOH)–streptavidin complex. Wide dashed lines indicate approximate positions of the Phe, Ser, Asn and Thr residues which are poorly defined in the electron-density maps. Similarly, a thinner dashed line shows the position of poorly defined residues 46–51.

ureido group, a polar interaction between biotin sulfur and the hydroxyl group of Thr90, and hydrogen-bonded interactions with the valeryl carboxyl group that includes a hydrogen bond from the backbone NH of Asn49, which is situated in a flexible loop in unliganded streptavidin that becomes ordered on biotin binding.

Previous work suggests that in addition to good packing interactions, several additional factors contribute to the exceptional affinity between biotin and streptavidin (Weber *et al.*, 1989). These include stabilization of a biotin resonance form whose urea O atom is more negatively charged than in aqueous solution, so that the urea O atom can make three hydrogen bonds of precise geometry to donors forming an 'oxyanion pocket' when bound to the protein, *versus* the two hydrogen bonds accepted by the sp^2 urea O atom from water molecules in solution. Although several water molecules are displaced from unliganded streptavidin on biotin binding, including a molecule bound with high occupancy in the ureido O atom 'oxyanion pocket', most residues that hydrogen bond to the biotin are geometrically preorganized in the unliganded streptavidin structure. An exception is a loop that forms a hydrogen bond with the biotin valeryl carboxyl as outlined above.

Thermodynamic measurements (Weber, Wendoloski *et al.*, 1992) of biotin binding to streptavidin show that the process is driven predominantly by a large favorable change in enthalpy (Table 1). In addition to non-specific packing interactions, the major component of the favorable enthalpy change is most likely associated with the ability of the highly polarizable biotin ureido group to form an additional hydrogen bond when bound to the protein that it does not form in solution.

In the crystal structure of the biotin-fluorescein (BTF)–streptavidin complex, electron density for the biotin portion of the ligand is well defined and shows that interactions between the biotin and streptavidin seen in the biotin–streptavidin complex (including the hydrogen bond from the backbone NH of Asn49 to an analogous carbonyl O atom of the amide linkage between biotin and fluorescein) are essentially maintained (Fig. 2*b*). Although the biotin portion of BTF ligand is well defined, only the positions of four methylene C atoms of the linker are defined in the electron-density maps. The isotropic B values, which indicate the extent of atomic motion, become increasingly large along the linker in the direction away from the bound biotin so that beyond the fourth methylene linker group, the remainder of the linker and the fluorescein macrocycle are not visible in the electron-density maps. However, comparison of electron-density maps of the biotin–streptavidin and BTF–streptavidin complexes shows that some five to six water molecules whose electron density is well defined in the biotin–strepatvidin complex are not observed in the BTF–streptavidin complex. This result suggests that the fluorescein and linker atoms are statically or dynamically disordered along the protein surface but are nevertheless able to displace bound water molecules.

Although definitive titration calorimetric data is not available for BTF–streptavidin complex formation, free-energy estimates derived from differential scanning calorimetric experiments suggest that BTF binds approximately four times more tightly than biotin itself (Table 1).

HABA–streptavidin interactions

Crystallographic studies show that HABA binds with the benzoic acid portion at the bottom of the biotin-binding pocket and with one edge of the hydroxyphenyl ring buried in the protein interior and the other partially exposed to solvent (Fig. 2*c*). A key ionic interaction between ligand and protein is made by one of the dye carboxylate O atoms which is situated in a pocket formed by three hydrogen-bond donating groups, Tyr43, Asn23 and Ser27, whose side chains are oriented to optimally stabilize a tetrahedral oxyanion formed by the biotin ureido group in the biotin–streptavidin complex (Weber *et al.*, 1989; Weber, Wendoloski *et al.*, 1992). Spectroscopic indicators show that HABA binds to streptavidin in the hydrazone form where a proton is transferred from the terminal phenyl hydroxy group to the diazo N atom proximal to the carboxyphenyl ring (Thomas & Merlin, 1979; Mahmoud, Ibrahim & Hamed, 1983). The hydrazone NH proton participates in a hydrogen-bond network with the second HABA carboxylate O atom and the hydroxyl group of Ser45. The phenylbenzoic acid ring packs in a hydrophobic pocket formed by side chains of Thr90 and tryptophan residues 92 and 108, and the side chain of Trp120 from a diad-related subunit of the tetramer. The phenylbenzoic acid ring packs perpendicular to the Trp108 indole side chain to form a favorable interaromatic ring edge-to-face interaction. The hydroxyphenyl ring is sandwiched between the aromatic ring of Trp79 at the base of the pocket and loop residues 48–51. Residues of this loop are disordered in apostreptavidin structure and well ordered in the biotin–streptavidin complex owing to hydrogen-bond formation between one of the biotin carboxylate O atoms and the backbone NH of Asn49 (Weber *et al.*, 1989). In the HABA–streptavidin complex, the loop is partially ordered owing to packing interactions between ligand atoms and loop residues.

Thermodynamic measurements of HABA–streptavidin binding show that it binds some ten orders of magnitude less tightly than biotin and that the interaction energetics are dominated by favorable entropy components. Consequently, both hydrazone formation and the extensive hydrogen-bond network with the protein which result on HABA binding appear to reflect an energetic accommodation that may compensate for solution hydrogen bonds formed with

the ligand and confer some binding specificity, but not stability, on complex formation. Instead, ligand desolvation or other entropic factors appear to dominate the energetics of HABA binding.

Several modified forms of HABA were synthesized and characterized as part of a program to develop diagnostic reporter dyes with improved binding affinity for streptavidin. The structure of one of these derivatives, 3′,5′-dimethyl-HABA, complexed to streptavidin is shown in Fig. 2(*d*). Relative to the bound conformation of HABA, 3′,5′-dimethyl-HABA shows a large movement of the hydroxyphenyl ring and loss of the Tyr54-to-water hydrogen bond. Comparison of the electron-density maps of HABA and 3′,5′-dimethyl-HABA complexed with streptavidin shows that the latter ligand is relatively disordered in the binding pocket.

Thermodynamic studies of 3′,5′-dimethyl-HABA binding show that it binds almost three orders of magnitude more tightly than HABA and that virtually all of the increase in ligand-binding free energy comes from favorable entropy gains (Table 1). These are attributable to enhanced desolvation, the displacement of an additional water molecule relative to HABA and the retention of some ligand conformational flexibility on binding.

Streptavidin–peptide interactions

Only the central His-Pro-Gln residues of the seven residue peptide (NH_2-Phe-Ser-His-Pro-Gln-Asn-Thr-COOH) soaked into the streptavidin crystals are clearly visible in the electron-density maps (Weber, Pantoliano *et al.*, 1992). The tripeptide sequence His-Pro-Gln binds in a compact conformation where the histidine and glutamine side chains form a loop closed by hydrogen bonding to a water molecule. The water molecule makes an additional hydrogen bond to Asp128 of the protein, while the peptide histidine Nδ1 N atom donates a hydrogen bond to the side-chain O atom of Thr90 (Fig. 2*e*). The glutamine and histidine side chains of the peptide show lower isotropic temperature factors than their backbone atoms, including the entire proline. This suggests that the hydrogen-bonding network extending from Thr90, through the peptide histidine side chain and the immobilized water to Asp128 fixes the peptide in place at the biotin-binding site.

Titration calorimetry studies show that the heptapeptide binds streptavidin with nearly the same affinity as HABA, although the energetic contributions are completely different (Table 1). Most notable in the case of the peptide binding is the net large and favorable enthalpy of binding, which is however, largely compensated by a large unfavorable entropy component. Favorable enthalpy components could arise from the extensive hydrogen-bonding network that accompanies peptide binding and necessitates only a small structural reorganization of a tightly bound water molecule bound in the oxyanion pocket of unliganded streptavidin. A probable source of the large unfavorable entropy is the necessity to freeze out numerous internal conformational degrees of freedom on peptide binding. These effects are apparently well in excess of any favorable entropy contributions arising from ligand desolvation or water displacement from the binding site.

Discussion

These studies reveal several points that are relevant both to a fundamental understanding of the thermodynamics of protein–ligand interactions and the practical application of structure-based drug design.

(1) High-affinity ligand interactions frequently involve electronic reorganization of the ligand to enhance interactions with the protein-binding site. This is seen both in biotin binding to streptavidin, where a biotin resonance form that allows additional hydrogen bonding is bound and in HABA binding, where a hydrazone tautomer of the free molecule is bound. This characteristic of ligand binding is of course shared with most enzyme substrates, where induced electronic reorganization of the substrate manifests itself as transition-state stabilization. Although enzyme transition states have high energy, transition-state analogs that can readily assume the geometric and electronic configuration of the substrate transition state typically constitute very potent inhibitors. It is notable that since the pairwise potential functions incorporated in most molecular mechanics and dynamics programs assume fixed atomic charges, some of the most important physical contributions to ligand binding are omitted in such calculations. It is consequently unrealistic to expect these approaches to yield accurate estimates of binding energy when polarizable ligands are involved.

(2) Similar patterns of hydrogen bonding shared among different ligands give no real indication of the ligand-binding affinities, or of the dominant thermodynamic driving force for ligand association. Despite the fact that biotin and HABA are relatively similar in terms of molecular weight, flexibility and hydrogen-bonding interactions with streptavidin, the former binding is driven by enthalpy and the latter by entropy changes that occur on complex formation. These results suggest that while hydrogen-bonding interactions make major contributions to biotin binding, what appear to be relatively similar interactions for HABA are primarily compensating for lost solvent interactions. In summary, the free energy of ligand binding can be very different for ligands that may look similar in their structural interactions with the target receptor

(3) HABA and the screened peptide (NH_2-Phe-Ser-His-Pro-Gln-Asn-Thr-COOH) represent two naive ligands (by naive we mean ligands which presumably have not encountered this binding site in nature) that have very different, structures, molecular weights and hydrogen-bonding capabilities. These differences are re-

flected in different enthalpy and entropy contributions to binding free energy, although the net free-energy differences for the two ligands are similar. In summary, the free energy of ligand binding can be very similar for ligands that may look very different in their structural interactions with the target receptor.

(4) Many high-affinity ligand interactions that result from strong bond formation reflect highly favorable enthalpy contributions to binding free energy. These interactions also tend to produce structurally well defined ligand positions as exemplified by low isotropic temperature factors seen for biotin. However, some ligands that show favorable entropy contributions to ligand binding show significant disordering effects that may be reflected in some residual static or dynamic ligand disorder when bound and/or displacement of water molecules which are rotationally or translationally restricted ('immobilized') on the protein surface in the absence of bound ligand. This effect is seen both in the enhanced binding of the biotin–fluorescein conjugate and the 3′, 5′-dimethyl-HABA derivatives. Both modified ligands have substituent parts that are more disordered than the parent ligands, displace 'immobilized' water molecules at the protein surface and have higher binding constants than corresponding parent ligands. In the case of the 3′,5′-dimethyl-HABA derivative, it was quantitatively possible to show that the enhanced binding of this compound relative to HABA was due to a favorable entropy effect on binding free energy.

(5) Screening with flexible diversity libraries like polypeptides allows the sampling of a very large number of conformations with low-lying energy states, one of which may be able to form favorable energetic interactions with a naive receptor binding site. Although the binding energetics of these ligands can be reasonably favorable, as in the case of the screened peptide (NH_2-Phe-Ser-His-Pro-Gln-Asn-Thr-COOH) bound to streptavidin, there are large entropy costs associated with freezing out flexible solution conformational states. Consequently, it is clear that the best way to realize the potential of these flexible 'sampling' ligands is to determine their bound structures and then use this information to rigidify the structure. Rigidification, in fact, is a common strategy for improving drug lead binding in analog drug elaboration. However, lacking structural data, this strategy becomes very difficult to execute as the lead ligand becomes as large and flexible as a tetrapeptide.

An additional feature that can be exploited to potentially enhance ligand-binding affinity, through a reduction in both ligand and solvent entropy, is to produce cyclic structures that mimic both the flexible side chains of the ligand and any sequestered water molecules, as for example seen to form key interactions in the streptavidin–peptide complex (Weber, Pantoliano *et al.*, 1992). Clearly, without three-dimensional structures of such bound leads, it is difficult to infer the correct ring-linkage geometry and impossible to infer the key role of water molecules in screened ligand binding.

In summary, a series of structural and thermodynamic observations have been described which emphasize the diversity of potential strategies for improving ligand binding affinity. Many of these strategies find straightforward parallels in conventional structure–activity relationship approaches to drug design. A simple example is rigidification of a ligand to reduce the loss of solution conformational entropy when binding, a situation necessitated, for example, when the bound ligand is able to effect multiple geometrically precise hydrogen-bonding interactions with a receptor. Less obvious are the situations where entropic stabilization occurs through retention of some ligand disorder on binding, together with the concomitant displacement of 'immobilized' solvent from the protein surface.

References

Appelt, K., Bacquet, R. J., Bartlett, C. A., Booth, C. L. J., Freer, S. T., Fuhry, M. A. M., Gehring, M. R., Herrmann, S. M., Howland, E. F., Janson, C. A., Jones, T. R., Kan, C.-C., Kathardekar, V., Lewis, K. K., Marzoni, G. P., Matthews, D. A., Mohr, C., Moomaw, E. W., Morse, C. A., Oatley, S. J., Ogden, R. C., Reddy, M. R., Reich, S. H., Schoettlin, W. S., Smith, W. W., Varney, M. D., Villafranca, J. E., Ward, R. W., Webber, S., Webber, S. E., Welsh, K. M. & White, J. (1991). *J. Med. Chem.* **34**, 1925–1934.

Brandts, J. F. & Lin, L.-N. (1990). *Biochemistry*, **29**, 6927–6940.

Chaiet, L. & Wolf, F. J. (1964). *Arch. Biochem. Biophys.* **106**, 1–5.

Devlin, J. J., Panganiban, L. C. & Devlin, P. E. (1990). *Science*, **249**, 404.

Erion, M. D., Niwas, S., Rose, J. D., Anathan, S., Allen, M., Secrist, J. A. III, Babu, Y. S., Bugg, C. E., Guida, W. C., Ealick, S. E. & Montgomery, J. A. (1993). *J. Med. Chem.* **36**, 3771–3783.

Finzel, B. C. (1987). *J. Appl. Cryst.* **20**, 53–57.

Green, N. M. (1965). *Biochem. J.* **94**, 23c–24c.

Green, N. M. (1975). *Avidin.* In *Advances in Protein Chemistry*, edited by C. B. Anfinsen, J. T. Edsall & F. M. Richards, pp. 85–133. New York: Academic Press.

Hendrickson, W. A. & Konnert, J. H. (1980). In *Biomolecular Structure, Function, Conformation and Evolution*, edited by R. Srinivasan, pp. 43–57. Oxford: Oxford Univ. Press.

Howard, A. J., Gilliland, G. L., Finzel, B. C., Poulos, T. L., Ohlendorf, D. H. & Salemme, F. R. (1987). *J. Appl. Cryst.* **20**, 383–387.

Jones, T. A. (1978). *J. Appl. Cryst.* **11**, 268–272.

Kraulis, P. J. (1991). *J. Appl. Cryst.* **24**, 946–950.

Lam, K. S., Salmon, S. E., Hersh, E. M., Hruby, V. J., Kazmierski, W. M. & Knapp, R. J. (1991). *Nature (London)*, **354**, 82–86.

Mahmoud, M. R., Ibrahim, S. A. & Hamed, M. A. (1983). *Spectrochim. Acta A*, **39**, 729–733.

Pahler, A., Hendrickson, W. A., Kolk, M. A. G., Argarana, C. E. & Cantor, C. R. (1987). *J. Biol. Chem.* **262**, 13933–13937.

Thomas, E. W. & Merlin, J. C. (1979). *Spectrochim. Acta A*, **35**, 1251–1255.

Weber, P. C., Ohlendorf, D. H., Wendoloski, J. J. & Salemme, F. R. (1989). *Science*, **243**, 85–88.

Weber, P. C., Pantoliano, M. W., Simons, D. M. & Salemme, F. R. (1994). *J. Am. Chem. Soc.* **116**, 2717–2724.

Weber, P. C., Pantoliano, M. W. & Thompson, L. D. (1992). *Biochemistry*, **31**, 9350–9354.

Weber, P. C., Wendoloski, J. J., Pantoliano, M. W. & Salemme, F. R. (1992). *J. Am. Chem. Soc.* **114**, 3197–3200.

Wiseman, T., Williston, S., Brandts, J. F. & Lin, L. (1989). *Anal. Biochem.* **179**, 131–137.